

Pre-discovery observations of CoRoT-1b and CoRoT-2b with the BEST survey

H. Rauer¹, A. Erikson, P. Kabath, P. Hedelt

DLR, Institut für Planetenforschung, Rutherfordstr. 2, 12489 Berlin, Germany

M. Boer

Observatoire de Haute Provence, St Michel-l'Observatoire, 04870, France

L. Carone

Rheinisches Institut für Umweltforschung, Universität zu Köln, Abt. Planetenforschung,
Aachener Str. 209, 50931 Köln, Germany

Sz. Csizmadia

DLR, Institut für Planetenforschung, Rutherfordstr. 2, 12489 Berlin, Germany

P. Eigmüller

Thüringer Landessternwarte Tautenburg, Sternwarte 5, 07778 Tautenburg, Germany

P. v. Paris, S. Renner²

DLR, Institut für Planetenforschung, Rutherfordstr. 2, 12489 Berlin, Germany

G. Tournois

Observatoire de Haute Provence, St Michel-l'Observatoire, 04870, France

and

R. Titz, H. Voss³

DLR, Institut für Planetenforschung, Rutherfordstr. 2, 12489 Berlin, Germany

Received _____; accepted _____

¹TU Berlin, Zentrum für Astronomie und Astrophysik, Hardenbergstr. 36, 10623 Berlin, Germany

²Laboratoire d’Astronomie de Lille, Université de Lille 1, 1 impasse de l’Observatoire, 59000 Lille, France

³Departament d’Astronomia i Meteorologia, Facultat de Física, Universitat de Barcelona, C/ Martí i Franquès 1, 08028 Barcelona, Spain

ABSTRACT

The BEST wide-angle telescope installed at the Observatoire de Haute-Provence and operated in remote control from Berlin by the Institut für Planetenforschung, DLR, has observed the CoRoT target fields prior to the mission. The resulting archive of stellar photometric lightcurves is used to search for deep transit events announced during CoRoT's alarm-mode to aid in fast photometric confirmation of these events. The "initial run" field of CoRoT (IRa01) has been observed with BEST in November and December 2006 for 12 nights. The first "long run" field (LRc01) was observed from June to September 2005 for 35 nights. After standard CCD data reduction, aperture photometry has been performed using the ISIS image subtraction method. About 30,000 lightcurves were obtained in each field. Transits of the first detected planets by the CoRoT mission, CoRoT-1b and CoRoT-2b, were found in archived data of the BEST survey and their lightcurves are presented here. Such detections provide useful information at the early stage of the organization of follow-up observations of satellite alarm-mode planet candidates. In addition, no period change was found over ~ 4 years between the first BEST observation and last available transit observations.

Subject headings: Techniques: photometry - Planets and satellites: CoRoT-1b, CoRoT-2b

1. Introduction

The Berlin Exoplanet Search Telescope (BEST) is a 19.5 cm aperture wide angle telescope dedicated to time-series photometric observations (Rauer et al. 2004). The main purpose of the instrument is to provide ground-based support to the CoRoT space mission (CNES; (Baglin et al. 2006)). The mission target fields are observed at least one year prior to the observations of the spacecraft. Therefore, planetary transit candidates found by CoRoT at bright stars can be searched for quickly in the BEST archive to confirm the transit event and to check the ephemeris. In addition, BEST data sets are used to search for new variable stars in the CoRoT target fields which are input to the additional science program, like e.g. eclipsing binary stars ((Karoff et al. 2007), (Kabath et al. 2007), (Kabath et al. 2008)). Furthermore, information on variable stars nearby CoRoT transit candidates can be used to help disentangling crowding problems during the CoRoT lightcurve analysis.

The transit signals of the first two planets detected by CoRoT (CoRoT-1b and CoRoT-2b) ((Barge et al. 2008), (Alonso et al. 2008)), were found using the "alarm detection mode" of the mission, during ongoing observations of the respective target fields. Since both planets orbit relatively bright stars, we searched for signatures of the transit candidates in our BEST data archive. Partial transit events of the planets were recorded by BEST in December 2006 and summer 2005 during observations of the CoRoT "initial run" and first "long run" fields. In the following, we describe these pre-discovery observations of CoRoT-1b and CoRoT-2b.

2. The BEST System

2.1. Telescope and Instrumentation

The observations were performed with the Berlin Exoplanet Search Telescope (BEST) system (Rauer et al. 2004). The BEST Telescope is a commercial flatfield telescope with 19.5 cm aperture and $f/2.7$ focal ratio and is mounted on a German equatorial mount. The system uses an air cooled Apogee-10 CCD camera with 2048×2048 pixels and a pixel scale of 5.5 arcsec/pixel, resulting in 3.1×3.1 square degree field of view (FOV). The readout time of the CCD is 9s and the saturation level is reached with 16384 ADU. In order to detect as many photons as possible no filters are used. Guiding of the telescope is performed by a 9 cm aperture telescope equipped with a ST-4 CCD camera.

The BEST system is located at the Observatoire de Haute-Provence (OHP), France, since 2004. During the commissioning phase of the BEST telescope for the OHP site, the system was upgraded to allow remote control of all its components as well as a system and environment monitoring. In autumn 2006 the first observations in remote control mode were performed by an observer at DLR in Berlin. Since then, the system is controlled from Berlin with occasional technical service visits at OHP. The remote observer starts the system at the beginning of the night and operates until the target field is acquired. Then, automatic exposure sequences are taken throughout the night. The DLR staff cooperates with local Berlin amateur astronomers who participate in the remote observations.

Observations are obtained for typically 30,000 stars in a target field. The reduced stellar lightcurves are archived for subsequent analysis.

2.2. Data Center and Archiving

In order to process the observational data acquired with the BEST telescope sufficiently fast, a dedicated data processing center consisting of a computer cluster system was installed at DLR during spring 2006. The data processing center consists of 18 calculation nodes and 3 Tb disk space in total.

The BEST stellar lightcurves data base contains stellar coordinates, time of observation, magnitude and magnitude error of the individual measurements for each detected star within the BEST fields. To allow a first estimate of stellar variability in the lightcurves a variability index calculated according to (Zhang et al. 2003) has been included. The content of the data base is available to the scientific community upon request.

3. Observations

In the following we describe the data obtained on the CoRoT IRa01 and LRc01 stellar fields which were used to check the transit candidates of the later confirmed planets CoRoT-1b and CoRoT-2b.

3.1. General Observing Modes

The CCD is cooled to its operational temperature around 20°C below outdoor temperature. Due to the location in Haute-Provence the outdoor temperature changed over the seasons with extreme values between -10°C to $+20^{\circ}\text{C}$. However, variations during the observations were mostly limited to a couple of degrees once stabilized during the astronomical night. Calibration bias frames and dome flatfields are acquired at the beginning of each night.

The general scientific observing sequence consists of a series of a 40 sec exposures followed by a 240 sec exposure. Dark frame images are taken every 25 minutes with the same exposure time as the science images. This fully automatized sequence takes about 30 minutes. The resulting duty cycle for the scientific images on an average good night is around 50-60 %. The dark and bias frames acquired within the observing session are used to monitor the performance of the CCD over the night. At the end of the observing runs, additional bias and dark frames are taken for calibration purposes.

3.2. BEST Data Sets of the CoRoT Fields IRa01 and LRc01

The IRa01 field was observed in 12 nights spread over a period of 40 days from 11th November to 21th December 2006 (Kabath et al. 2007). The LRc01 field was observed from 6th June until 7th Sept 2005 in 35 nights spread over 89 days (Karoff et al. 2007). No observations were performed 6 days around full Moon. Additional data gaps resulted from bad weather conditions at OHP.

The observed CoRoT IRa01 field is located at $RA = 06^h57^m18^s$ and $Dec = -01^\circ42'00''$ ($J2000.0$) (Michel et al. 2006). The BEST FOV covered the CoRoT exoplanetary field only to avoid the bright stars in the CoRoT asteroseismology field. The BEST FOV, therefore, was centered at $RA = 06^h46^m24^s$ and $Dec = -01^\circ54'00''$ ($J2000.0$).

The CoRoT LRc01 field is located at $RA = 19^h23^m33^s$ and $Dec = +00^\circ27'36''$ (Michel et al. 2006). Again, the BEST FOV was offset to avoid the bright asteroseismology target stars and was centered at $RA = 19^h00^m00^s$ and $Dec = +00^\circ01'55''$.

Since the CoRoT fields are located near the celestial equator they can be observed only at relatively low altitudes (< 50 degree) from OHP. Therefore, the BEST data set had to be obtained at relatively high airmass. Typically observation arcs ranged between 3-6 hours

per night.

In this paper we analyze the images acquired with 240 seconds exposure time since they provide an overlap with the CoRoT magnitude range with sufficient photometric precision. The data sets contain in total 300 frames for the IRa01 field and 727 frames for the LRc01 field. The magnitude range of the detected stars in the BEST fields (about 30000) is 10 mag to 18 mag and thus overlaps with the CoRoT magnitude range (12 – 16 mag). Typically, during a good photometric night BEST acquires lightcurves with a precision $\leq 1\%$ for 3000-4000 stars in the range 10 – 13 mag.

4. BEST Data Reduction Pipeline

The BEST data reduction pipeline includes the basic CCD imaging reduction steps, such as dark current and bias subtraction as well as flatfielding, which have been performed by computing the related master frames for each night ((Rauer et al. 2004), (Voss 2006)). For the photometric data reduction we used the ISIS image subtraction method. A detailed description of the ISIS method can be found in (Alard 2000).

In a first step, the stellar coordinates in every image are interpolated with respect to a single chosen reference frame from the middle of the observation run. For this purpose the matching routine `interp` from the ISIS package (Alard 2000) was used. In this way slight translations are well corrected and a coordinate template common to all images is created.

In a second step, the ISIS image subtraction method is applied to remove background contaminat to the stellar light. This is done by subtracting a reference frame from all the scientific frames thereby leaving only the remaining variability of each star as the final product. In this process all frames have to match to the same seeing. The used reference frame is created from typically the 10 best seeing images obtained during the whole

observation campaign. This reference frame is thereafter subtracted from all other images, such that the stellar PSF on the reference frame is convolved with the corresponding stellar PSFs on the scientific images to best match the stellar PSFs in each individual frame. To obtain the flux variation of each star as a function of time, aperture photometry is applied on the reference frame and on all convolved and subtracted frames. The magnitude of each star was determined by aperture photometry in the reference frame. The magnitude at each time step was then determined by adding the deviations from the reference which were determined using the same aperture in the individual difference frames. The implementation of the BEST data pipe line is described in (Karoff et al. 2007). Discussions on the obtained photometric quality for the CoRoT fields IRa01 and LRc01 can be found in (Kabath et al. 2007) and (Karoff et al. 2007). A local extinction correction is performed within the ISIS package that significantly reduces the influence of differential extinction present due to the large FOV. We use a fixed aperture of 7 pixels to match the FWHM range between 1 – 3 pixels of the analyzed stars as discussed in (Karoff et al. 2007).

In the last step the (x,y) coordinates of the CCD frames are transformed into right ascension and declination. For such astrometric transformation we compared the 300 brightest stars in the BEST data set with the USNO-A2.0 catalog using the MATCH routine (Valdes et al. 1995) to determine the transformation parameters. Thereafter the transformation of the full BEST data set was performed and the corresponding sub-set of stars in the USNO-A2.0 identified. A more detailed description of the approach can be found in (Kabath et al. 2007) and (Karoff et al. 2007). Using these stars we calculated the shift in magnitude with respect to the USNO-A2.0 catalog. Since only the relative magnitudes are needed to identify the variable stars we do not intend to perform real absolute photometric calibration.

The data can be affected by systematic errors due to zero point offsets from night to

night or large systematic trends due to variable weather conditions. In order to remove such trends, we apply a routine by (Tamuz et al. 2005) four times on both data sets. A more detailed analysis of the effect of systematic errors for the whole BEST data set is under investigation.

5. Results

5.1. Photometric pre-discovery observations of CoRoT-1b and CoRoT-2b

The two planets CoRoT-1b and CoRoT-2b were discovered by the CoRoT space mission in the "alarm mode" during observations of its "initial run" (IRa01) and the first "long run" (LRc01) fields ((Barge et al. 2008) and (Alonso et al. 2008)). The planets orbit relatively bright stars ($V=13.6$ mag for CoRoT-1b and $V=12.57$ mag for CoRoT-2b) but within the magnitude range covered by BEST. Furthermore, their transits are strong signals of more than 2 % and 3% depths, respectively. We therefore searched for signatures of the transit candidates in our BEST data archive, based on the determined transit epochs from the CoRoT alarm-mode operations. The star and planet parameters for CoRoT-1b and CoRoT-2b are given in Table 1.

The BEST archive data sets of the respective fields include 12 nights for the IRa01 and 35 nights for the LRc01 field. Figure 1 shows the target stars and their near vicinity. CoRoT-1b is located in a very crowded part of the CoRoT field. As a consequence, using the normal data pipeline with a photometric aperture of seven pixels, resulted in a diluted signal where a neighbouring star contributed to the total flux within the aperture. To minimize this effect, manual photometry with an aperture size of five pixels was performed in order to obtain optimum photometric accuracy. In all other aspects the reduction for CoRoT-1b was performed as outlined in the previous section. CoRoT-2b was processed

using the standard BEST pipeline.

Due to the restricted data set, only one partial transit event of CoRoT-1b was covered by BEST observations. Figure 2 shows the lightcurve obtained for CoRoT-1b on 10 December 2006. Only the egress of the transit event could be covered at the beginning of the night. The data set is severely affected by noise due to the weather situation. In addition, the star is located at the fainter end of the BEST magnitude range for signals of the CoRoT-1b order. Nevertheless the transit signature can be seen in the data. For comparison another star of similar magnitude in the vicinity is also presented in the figure.

Figure 3 shows the composite lightcurve obtained on CoRoT-2b by BEST. In total, three transit events could be covered in the observing period from June to September 2005. Again, the data quality varies from night to night due to the weather situation, and on two nights only partial transits could be obtained. However, an almost complete transit signal is detected on 14 July 2005. Phase folding of the lightcurves from the individual nights has been done using the epochs and orbital period determined from the CoRoT data (see Table 1). For comparison another star is also presented in the figure. A good agreement was found in orbital period and transit shape between the events detected by BEST and the more detailed CoRoT observations.

In both cases the pre-discovery observations of CoRoT-1b and CoRoT-2b with the BEST survey were used during CoRoT follow-up observations to refine early ephemeris and optimize the effort to confirm their planetary nature ((Barge et al. 2008) and (Alonso et al. 2008)). The lightcurve data used in this paper are given in Tables 3 and 4.

5.2. Detailed Analysis of a CoRoT-1b transiting event

In our data set we found a partial transit event of CoRoT-1b (Figure 2). The data points cover the egress event. This observation of a transit was obtained 60 days before the discovery observations by the CoRoT satellite. We therefore tried to constrain the midcenter time to obtain an additional point for an O-C analysis.

For this purpose we fixed the stellar, planetary and orbital parameters at values given in (Barge et al. 2008). The only free parameter was the midtime of the transit. The cycle number at the time of observations was -53 , and therefore the predicted time of the transit is HJD 2 454 079.4785. **We scanned the region around this predicted time (± 4 hours) with a step size of 0.5 seconds to find the best agreement between the model and the observed lightcurves.** Instead of the original light curve we used a smoothed light curve, applying a 2-points moving average **in order to increase the SNR**. The resulting midcenter time of the transit was found to be $T_{\text{mid}}(\text{HJD}) = 2\,454\,079.4673 \pm 0.0088$. The $O - C$ value corresponds to $O - C = -0.0112 \pm 0.0088$ days. The $O - C$ value determined from this partial light curve therefore is zero within the 3σ error bars, and we conclude that our observation is in agreement with the ephemeris of (Barge et al. 2008).

5.3. Detailed Analysis of CoRoT-2b transiting events

Our transit observations of CoRoT-2b were obtained 2 years prior the discovery, therefore we can extend its $O - C$ diagram which is the base of the period studies.

The determination of the midtransit times can be done by fitting the light curves of individual transit events, but there can be at least three approaches: (1) fitting every parameters, (2) fitting every parameters except the period, or (3) fitting only the midtransit times. The first method - fitting all the parameters - could not be applied here because

we did not have enough data points to determine the epoch and period only from our observations. The second and third method (fitting everything except period which is fixed) were tried.

We chose the quadratic limb-darkened model of (Mandel and Agol 2002) who gave analytic expressions for the light loss of the system. In this model the planet is dark without observable radiation while the stellar disc is limb-darkened and both objects are spherical. This model has seven free parameters: orbital inclination, radius of the planet and the size of the semi-major axis (both of them is expressed in stellar radius unit), two limb darkening coefficients, the period and the epoch.

To find the best agreement between the model and the data a Markov Chain Monte Carlo method complemented with the Metropolitan-Hastings algorithm (see e.g. (Croll 2006)) was used.

In Figure 3 we show the results of both fitting approaches. The "long dash" line represents the model for the CoRoT data from Alonso et al. (2008), only the midtransit time was adjusted. The "long-short dash line" represents the fitted model to the BEST data where only the period was fixed at the value given in Alonso et al. (2008). In the descending and ascending branch of the transit the agreement is perfect but at the bottom part of the transit there is a small deviation. This deviation is caused by the different values of limb-darkening coefficients. These coefficients were fitted in (Alonso et al. 2008) and in our case. The CoRoT and BEST light curves have a different number of data points and different accuracies and hence we cannot determine these coefficients from the BEST lightcurves with such high accuracy as (Alonso et al. 2008). However, the semi-major axis and planet radius are in reasonable good agreement and the inclination differs by only 2.5 degrees. This good agreement in the planet to star radii ratio and semi-major axis is due to the fact that the lightcurves at this photometric accuracy level are not too sensitive

to the limb-darkening (Southworth 2008). This comparison illustrates that the data from ground-based surveys can be used for a realistic estimation of the planet parameters of detected exoplanets.

5.4. $O - C$ Analysis of CoRoT-2b

Our observations of CoRoT-2b were obtained almost 2 years prior to the CoRoT data. We, therefore, investigated whether a significant $O-C$ deviation could be detected in comparison to the ephemerides given in (Alonso et al. 2008). With these three new transits in total 15 observed transit timing data points are available for CoRoT-2b. The sources of the other 12 points are: one from (Alonso et al. 2008), one from (Vereš et al. 2009), and ten from the AXA working group (AXA: Amateur eXoplanets Archive, see: brucegary.net/AXA/x.htm).

To determine the mid-time of the observed transits, we fixed the model parameters at the values given in (Alonso et al. 2008) with the exception of the mid-time of the CoRoT transit. Only this parameter was adjusted to obtain an optimized fit of all observed transiting events. The corresponding $O - C$ values can be found in Table 2 and in graphical form in Figure 4.

The interpretation of this diagram is difficult because of two reasons. First, there is a lack of available observational data, which means that the $O - C$ is not well covered. Second, the precision of the published minima times allows only the study of large period changes.

The deviation of all $O - C$ values yielded $\chi^2 = 440$ when using the ephemeris of Alonso et al. (2008). A simple linear fit of the $O - C$ diagram yielded the following ephemeris:

$$T_{\min} (\text{HJD}) = 2454237.5357(16) + 1.7429861(58) \times E \quad (1)$$

With this ephemeris we reached $\chi^2 = 315$, and some improvement in the $O - C$ deviations. The new period value (1.7429861 days) is shorter than the one in (Alonso et al. 2008) by 0.9 ± 0.5 seconds. We conclude that there is no observable sign of period change in the available CoRoT-2b transit timing data. The lack of observed period change is in agreement with the results of (Alonso et al 2009). They analysed the transit times in the CoRoT data and found no clear sign of periodic period change which would have amplitudes larger than 10 seconds. However, (Alonso et al 2009) did not publish their individual $O - C$ data thereby preventing a direct comparison with our result. (Vereš et al. 2009) did also not find any sign of period variation on a shorter baseline of observations.

6. Summary

We present pre-discovery observations of the first two planets detected by the CoRoT space mission, CoRoT-1b and CoRoT-2b. The transit events were detected in the BEST data archive, based on the epochs determined from the CoRoT data ((Barge et al. 2008), (Alonso et al. 2008)). Although the observational duty cycle was severely affected by bad weather conditions, partial transits of both planets were detected by BEST. A transit of CoRoT-1b was observed on 10 December 2006. Transits of CoRoT-2b were observed in 14 July 2005, 28 July 2005 and 04 Aug 2005. No significant O-C deviation in comparison to the ephemerides of (Alonso et al. 2008) was found.

When planetary candidates are first announced from the CoRoT alarm-mode, their ephemeris can be based on few transit events only. At this point, confirmation from ground-based observations taken one or more years prior to the spacecraft observations aids in checking the ephemeris quickly. In addition, these observations confirm the transit on

the prime target and help identifying close possibly contaminating variable stars. We will continue to use the BEST data archive for this purpose in future to support the planet search in particular during the alarm-mode of CoRoT, when primarily deep transits around bright stars are detected which overlap with the detection range of BEST.

We are grateful to the enthusiastic support of our observations by Martin Dentel, Christopher Goldmann, Susanne Hoffman and Tino Wiese and during the data reduction and archiving phase by Christopher Carl, Sabrina Kirste and Mathias Wendt.

REFERENCES

- Alard, C. 2000, *A&AS*, 144, 363
- Alonso, R., Auvergne, M., Baglin, A., et al. 2008, *A&A*, 482, L21
- Alonso, R., Aigrain, S., Pont, F., Mazeh, T., & The CoRoT Exoplanet Science Team 2009, *IAU Symposium*, 253, 91
- Baglin, A., et al. 2006, 36th COSPAR Scientific Assembly, 36, 3749
- Barge, P., Baglin, A., Auvergne, M., et al. 2008, *A&A*, 482, L17
- Brown, T. M., Charbonneau, D., Gilliland, R. L., Noyes, R. W., & Burrows, A. 2001, *ApJ*, 552, 699
- Croll, B., 2006, *PASP* 118, 1351
- Kabath, P., et al. 2007, *AJ*, 134, 1560
- Kabath, P., et al. 2008, *AJ*, 136, 654
- Karoff, C., et al. 2007, *AJ*, 134, 766
- Mandel, K., Agol, E. 2002, *ApJ* 580, 171
- Michel, E., et al. 2006, *ESA Special Publication*, 1306, 473
- Rauer, H., Eislöffel, J., Erikson, A., Guenther, E., Hatzes, A. P., Michaelis, H., Voss, H. 2004, *PASP*, 116, 38
- Southworth, J. 2008, *MNRAS* 386, 1644
- Tamuz, O., Mazeh, T., & Zucker, S. 2005, *MNRAS*, 356, 1466
- Valdes, F. G., Campusano, L. E., Velasquez, J. D., & Stetson, P. B. 1995, *PASP*, 107, 1119

Vereš, P., Budaj, J., Világi, J., Galád, A., & Kornoš, L. 2009, Contributions of the
Astronomical Observatory Skalnaté Pleso, 39, 34

Voss, H. 2006, PhD Thesis, TU Berlin

Zhang, X.-B., Deng, L.-C., Xin, Y., & Zhou, X. 2003, Chinese Journal of Astronomy and
Astrophysics, 3, 151



Fig. 1.— Cut-outs (50×50 pixels each (**4.6×4.6 arcmin**)) of the surroundings of CoRoT-1b (left) and CoRoT-2b (right) in BEST data. The position of the targets is marked.

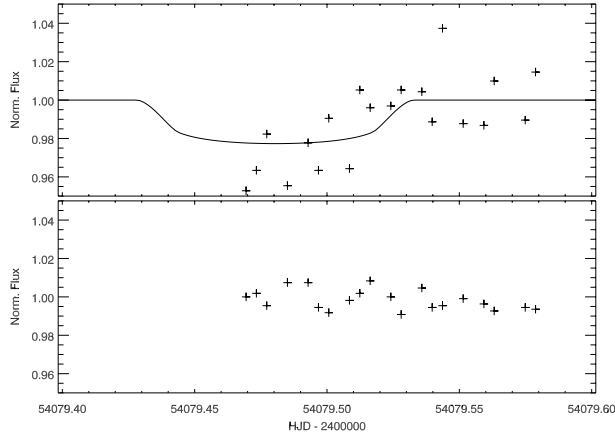


Fig. 2.— Top panel: BEST archive lightcurve of a transit event of CoRoT-1b obtained on 10 December 2006. The solid line indicates the transit shape according to CoRoT data (Barge et al. 2008). Lower panel: lightcurve of a nearby comparison star of similar magnitude.

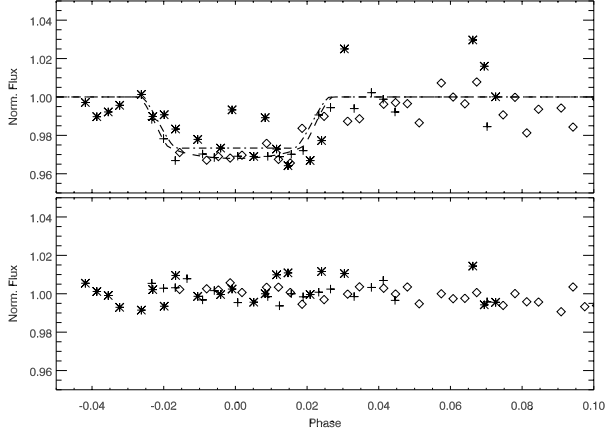


Fig. 3.— Top panel: BEST archive composite lightcurve of three transit events of CoRoT CoRoT-2b obtained on 14 July 2005 (+), 28 July 2005 (★) and 04 Aug 2005 (◇), respectively. Phase folding has been performed with $T_c[HJD] = 2454237.53562$ and $P[d] = 1.7429964$ determined from the CoRoT data (Alonso et al. 2008). The ”long dash” and ”long-short dash” lines indicate the transit shape according to CoRoT data (Alonso et al. 2008) and an independent fitting of the BEST data respectively. The residuals of the lightcurve fitting (0.009 mag) are in good agreement with the RMS (0.01 mag) of the BEST lightcurves. Lower panel: lightcurve of a nearby comparison star. Both stars have a similar magnitude as observed with BEST.

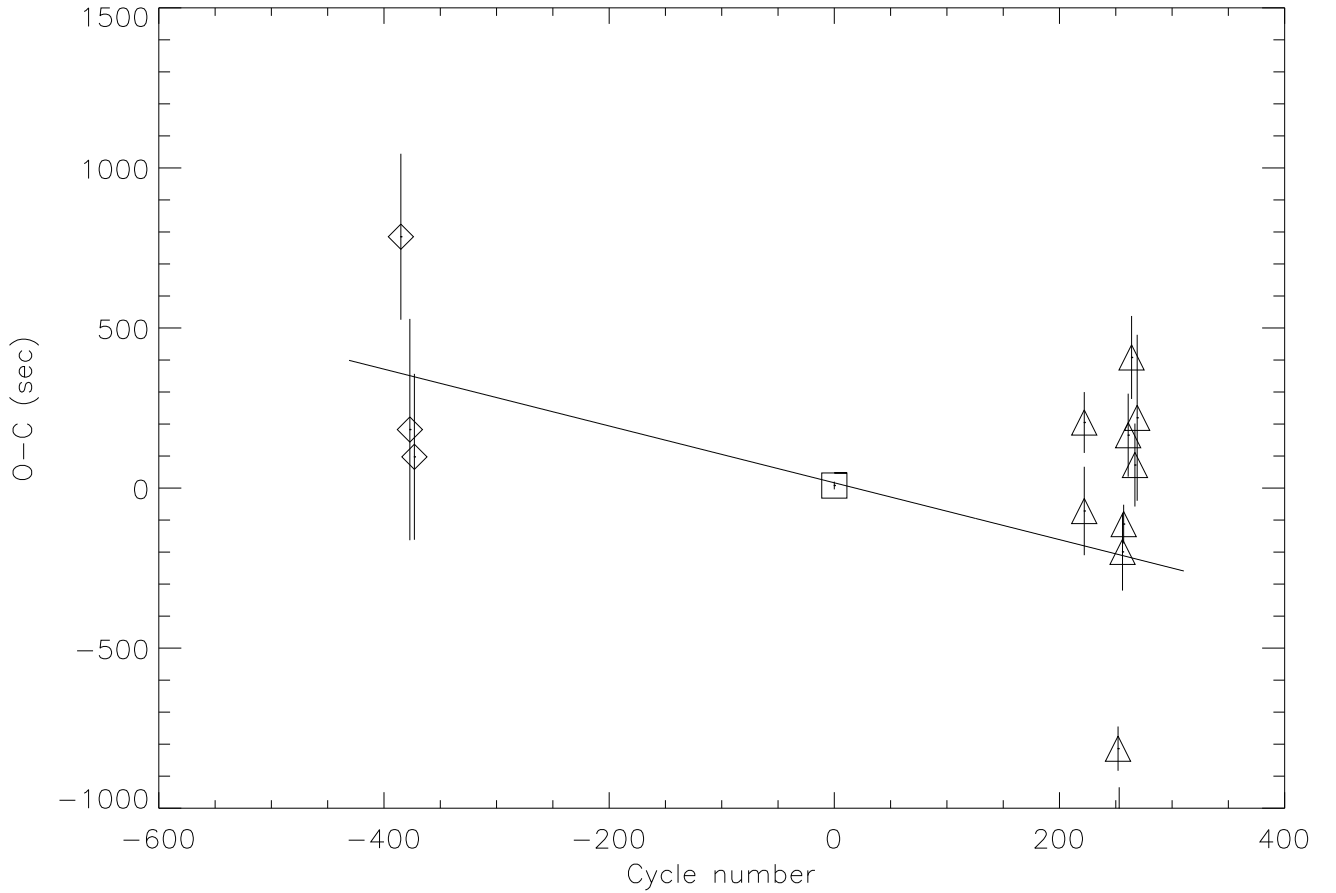


Fig. 4.— The $O - C$ diagram of CoRoT-2b with $O - C$ vs. cycle number. Vertical lines indicate the error bars. (\diamond) represents the BEST measurements, (\square) the data CoRoT data from (Alonso et al. 2008), while (\triangle) correspond to the observations from AXA and (Vereš et al. 2009). The solid line is a linear fit corresponding to Eq. 1.

Table 1: The star and planet parameters for CoRoT-1b and CoRoT-2b. The limb darkening coefficients u_+ and u_- are defined according to (Brown et al. 2001). All parameters in the lower part of the table are from (Barge et al. 2008) and (Alonso et al. 2008).

Parameters	CoRoT-1b	CoRoT-2b	
	(Barge et al. 2008)	(Alonso et al. 2008)	This paper
a/R_\star	4.92 ± 0.08	6.70 ± 0.03	6.32 ± 0.48
R_P/R_\star	0.1388 ± 0.0021	0.1667 ± 0.0006	0.1633 ± 0.0031
$i[deg]$	85.1 ± 0.5	87.84 ± 0.10	85.23 ± 1.37
u_+	0.71 ± 0.16	0.471 ± 0.019	-0.014 ± 0.28
u_-	0.13 ± 0.30	0.34 ± 0.04	0.024 ± 0.2
$RA[J2000.0]$	$06^h48^m19.17^s$	$19^h27^m06.5^s$	
$Dec[J2000.0]$	$-03^\circ06'07.78''$	$01^\circ23'01.5''$	
V_{mag}	13.6	12.57	
$P[d]$	1.5089557 ± 0.0000064	1.7429964 ± 0.0000017	
$T_c[HJD]$	2454159.4532 ± 0.0001	$2454237.53562 \pm 0.00014$	

Transit midtime (HJD)	N	O-C (days)	Reference
54706.4041 ± 0.0030	269	0.0024	(Vereš et al. 2009)
54702.9164 ± 0.0015	267	0.0007	AXA
54697.6913 ± 0.0015	264	0.0046	AXA
54692.4595 ± 0.0015	261	0.0018	AXA
54685.4843 ± 0.0007	257	-0.0014	AXA
54683.7403 ± 0.0014	256	-0.0024	AXA
54678.5016 ± 0.0012	253	-0.0121	AXA
54676.7612 ± 0.0008	252	-0.0095	AXA
54676.7577 ± 0.0010	252	-0.0130	AXA
54624.4831 ± 0.0011	222	0.0023	AXA
54624.4799 ± 0.0016	222	-0.0009	AXA
54237.53562 ± 0.00014	0	0.0000	(Alonso et al. 2008)
53587.399 ± 0.003	-373	0.001	This paper
53580.430 ± 0.004	-377	0.004	This paper
53566.498 ± 0.003	-385	0.016	This paper

Table 2: Transit observations and $O - C$ deviation of CoRoT 2b. The cycle number (N) is relative to $T_c[HJD] = 2454237.53562$ determined from the CoRoT data (Alonso et al. 2008).

Table 3: Observed normalized intensities of CoRoT-1. Intensity is from white light magnitudes, normalized to the out-of-eclipse light.

HJD-2454000	Intensity
79.47007	0.957
79.47448	0.967
79.47886	0.986
79.48326	0.959
79.49129	0.982
79.49562	0.967
79.50198	0.994
79.50636	0.968
79.51075	1.009
79.51516	1.000
79.52320	1.001
79.52760	1.009
79.53714	1.008
79.54152	0.993
79.54592	1.041
79.55030	0.992
79.55828	0.991
79.56269	1.014
79.57540	0.994
79.57973	1.019

Table 4: Observed normalized intensities of CoRoT-2. Intensity is from white light magnitudes, normalized to the out-of-eclipse light.

HJD-2453000	Intensity	HD-2453000	Intensity
566.44083	0.995	580.46740	0.985
566.44657	0.985	580.47851	1.032
566.45225	0.974	580.54095	1.037
566.45798	0.760	580.54656	1.023
566.46555	0.977	580.55205	1.007
566.47123	0.975	587.37038	0.979
566.48264	0.976	587.38350	0.974
566.49729	0.976	587.38918	0.976
566.50297	0.976	587.39491	0.976
566.50870	0.977	587.40071	0.977
566.51444	0.979	587.41267	0.983
566.52201	0.998	587.41841	0.975
566.52781	1.002	587.42415	0.973
566.53928	1.001	587.42988	0.991
566.54764	1.009	587.44063	0.997
566.55344	1.006	587.45204	0.995
566.55918	0.999	587.45784	0.996
566.60392	0.992	587.46962	1.004
580.35253	1.004	587.47535	1.005
580.35809	0.997	587.48109	1.004
580.36364	0.999	587.48689	0.994
580.36920	1.003	587.49763	1.015
580.37976	1.009	587.50337	1.007
580.38531	0.997	587.50911	1.004
580.39086	0.998	587.51484	1.015
580.39642	0.991	587.52766	0.998
580.40716	0.985	587.53346	1.007